MOLECULAR ONCOLOGY 7 (2013) 531–542

available at www.sciencedirect.com

SciVerse ScienceDirect

www.elsevier.com/locate/molonc

The High Mobility Group A proteins contribute to thyroid cell transformation by regulating miR-603 and miR-10b expression

Paula Mussnich[a,b], *Daniela D'Angelo*[a], *Vincenza Leone*[a], *Carlo Maria Croce*[c], *Alfredo Fusco*[a,*]

[a]*Istituto di Endocrinologia ed Oncologia Sperimentale del CNR, c/o Dipartimento di Biologia e Patologia Cellulare e Molecolare, Facoltà di Medicina e Chirurgia di Napoli, Università degli Studi di Napoli "Federico II", Naples, Italy*
[b]*CAPES Foundation, Ministry of Education of Brazil, Brasília DF 70040-020, Brazil*
[c]*Department of Molecular Virology, Immunology, and Medical Genetics, Comprehensive Cancer Center, Ohio State University, 460 West 12th Avenue, Columbus, OH 43210, USA*

ARTICLE INFO

Article history:
Received 17 September 2012
Received in revised form
7 January 2013
Accepted 8 January 2013
Available online 17 January 2013

Keywords:
microRNA
HMGA
Thyroid cells

ABSTRACT

The overexpression of the HMGA1 proteins is a feature of human malignant neoplasias and has a causal role in cell transformation. The aim of our study has been to investigate the microRNAs (miRNAs or miRs) regulated by the HMGA1 proteins in the process of cell transformation analyzing the miRNA expression profile of *v-ras-Ki* oncogene-transformed thyroid cells expressing or not HMGA1 proteins. We demonstrate that, among the miRNAs regulated by cell transformation, there are miR-10b, miR-21, miR-125b, miR-221 and miR-222 that are positively and miR-34a and miR-603 that are negatively regulated by HMGA1 expression. Then, we focused our attention on the miR-10b and miR-603 whose expression was dependent on the presence of HMGA1 also in other cell systems. We found that miR-10b is able to target the *PTEN* gene, whereas miR-603 targets the *CCND1* and *CCND2* genes coding for the cyclin D1 and cyclin D2 proteins, respectively. Moreover, functional studies showed that miR-10b and miR-603 regulate positively and negatively, respectively, cell proliferation and migration suggesting a role of their dysregulation in thyroid cell transformation.

1. Introduction

The High Mobility Group A (HMGA) family is composed of four proteins, HMGA1a, HMGA1b, HMGA1c, encoded by HMGA1 gene through alternative splicing, and HMGA2, encoded by the homonymous gene. The HMGA proteins bind the minor groove of AT-rich sequences. Their DNA-binding domain is located in the amino-terminal region of the protein and contains three short basic repeats, so-called AT-hooks (Reeves and Nissen, 1990). The HMGA proteins do not have transcriptional activity *per se*; however, they alter chromatin structure by interacting with the transcription machinery and, thereby, regulate, negatively or positively, the transcriptional activity of several genes (Abdulkadir at al., 1995; Lehming et al., 1994; Thanos et al., 1993; Thanos and Maniatis, 1992).

Overexpression of both the *HMGA* genes is a feature of malignant tumours. Indeed, they are widely expressed during embryogenesis and in malignant tumors (including pancreas, thyroid, colon, breast, lung, ovary, uterine cervix, prostate,

* *Corresponding author*. via Pansini 5, 80131 Napoli, Italy. Tel.: +39 081 7463602; fax: +39 081 2296674.
E-mail address: alfusco@unina.it (A. Fusco).
1574-7891/$ – see front matter © 2013 Federation of European Biochemical Societies. Published by Elsevier B.V. All rights reserved.
http://dx.doi.org/10.1016/j.molonc.2013.01.002

gastric carcinomas, squamous carcinomas of the oral cavity, head and neck tumors), whereas their expression is absent or very low in adult tissues (Fedele and Fusco, 2010; Fusco and Fedele, 2007). HMGA1 and HMGA2 protein expression is associated with a highly malignant phenotype. In fact, a significant correlation was detected between high levels of HMGA1 protein expression and the presence of lymph node metastasis and advanced clinical stage in colon carcinomas (Fusco and Fedele, 2007). The correlation between the levels of HMGA1 proteins and the malignant phenotype stimulated studies aimed to determine their role in the process of cell transformation and, in particular, to investigate whether their increase is a phenomenon peripherally associated with cell transformation or has a causal relationship with the malignant phenotype. Several studies indicate that both HMGA1 and HMGA2 proteins have oncogenic activities, being causally involved in neoplastic transformation. Indeed, blockage of hmga1 synthesis prevents rat thyroid cell transformation by murine transforming retroviruses (Berlingieri et al., 1995, 2002), and an adenovirus carrying the *HMGA1* gene in the antisense orientation induces apoptotic cell death in anaplastic human thyroid carcinoma cell lines, but not in normal thyroid cells (Scala et al., 2000). Moreover, the block of HMGA1 protein synthesis by antisense methodology or by shRNA reduces anchorage-independent proliferation in soft agar and increases the susceptibility to anoikis of lung and pancreatic carcinoma cells (Liau et al., 2007). Consistently, increased expression of both HMGA1 and HMGA2 proteins in several cell types induces anchorage-independent cell growth and ability to form both primary and metastatic tumors in athymic mice (Wood et al., 2000). Finally, transgenic mice overexpressing these proteins develop lipomas, NK-T/NK cell lymphomas and mixed growth hormone/prolactin pituitary adenomas at high frequency (Arlotta et al., 2000; Baldassarre et al., 2001; Fedele et al., 2002, 2005, 2011; Xu et al., 2004).

Recently, microRNAs have emerged as an important class of short endogenous RNAs that act as post-transcriptional regulators of gene expression. MiRNAs are small RNA molecules of 19-22-nt long deriving from double-stranded RNAs (dsRNAs). Currently, miRNAs are one of the most important regulatory molecules that modulate gene expression at post-transcriptional level by targeting mRNAs for direct cleavage or translation repression (Bartel, 2004). Since each miRNA is thought to regulate multiple genes, and hundreds of miRNA genes are predicted to be present in higher eukaryotes (Fabbri et al., 2008; Miska, 2005; Zamore and Haley, 2005), the potential regulatory circuitry afforded by miRNAs is enormous. Moreover, a large body of evidence suggests that miRNAs play a role in the etiology and pathogenesis of cancer by targeting oncogenes or tumor suppressor genes (Vandenboom et al., 2008).

Therefore, it is reasonable that HMGA1 proteins might affect cancer pathogenesis also by regulating the miRNA expression pattern to promote cell transformation. Then, we analyzed the miRNA expression profile of FRTL5, FRTL5-KiMSV and FRTL5-KiMSV-HMGA1as cells (Berlingieri et al., 2002). The FRTL5 are normal thyroid cells that do not express HMGA1 protein (Fusco et al., 1987). The FRTL5-KiMSV cells are FRTL5 transformed by the Kirsten murine sarcoma virus that induces, following cell transformation, the expression of the HMGA1 proteins and show a highly malignant phenotype (Fusco et al., 1987; Giancotti et al., 1987). The FRTL5-KiMSV-HMGA1as are FRTL5 transfected with a vector carrying the HMGA1 gene in an antisense orientation before being infected with the Kirsten murine sarcoma virus. These cells do not express the HMGA1 proteins, whereas they express significant levels of the retroviral transforming oncogene *v-ras-Ki* and do not depend on thyroid-stimulating hormone for the growth, but, in contrast with untransfected cells, do not grow in soft agar or form tumors in athymic mice (Berlingieri et al., 2002).

The miRNA expression profile of these cells showed that thirty miRNAs are upregulated with a fold-change higher than two, whereas eleven are downregulated, with the same fold-change as above, in the FRTL5-KiMSV cell line with respect to the normal FRTL5 cells. Among these miRNAs regulated by cell transformation, there are miR-10b, miR-21, miR-125b, miR-221 and miR-222, that are positively and miR-34a and miR-603, that are negatively regulated, by HMGA1 expression. We demonstrate that miR-10b targets the PTEN gene, whereas miR-603 targets the *CCND1* and *CCND2* genes, and that these miRNAs regulate, in opposite way, cell proliferation and migration.

2. Material and methods

2.1. *miRNACHIP microarray*

RNA labeling, hybridization on miRNA microarray chips and microarray analyses were performed as previously described. miRNAs were analyzed by class comparison using Student's t test procedure. Each sample was analyzed for miRNA expression profile in triplicate (Liu et al., 2004).

2.2. *RNA extraction, reverse transcription and quantitative real time (qRT)-PCR*

Total RNA was isolated from cells with Trizol (Invitrogen, Carlsbad, California, USA), according to manufacturer's instructions. 1 μg of RNA from each sample was reverse-transcribed with miScript reverse transcription Kit (Qiagen). The qRT-PCR for mature miRNA was performed according to miScript System Kits (Qiagen) instructions, a specific kit for miRNA quantification and profiling. Reactions contained miScript Primer Sets (Qiagen), specific for each analyzed miRNA and U6 (used to normalize RNA levels). qRT-PCR analyses for *CCND1*, *CCND2* and *PTEN* were performed using the primers reported in Supplementary Material (Supplementary Information). Each reaction was carried out three times in triplicate. To calculate the relative expression levels, we used the $2^{-\Delta\Delta CT}$ method (Livak and Schmittgen, 2001).

2.3. *Cells lines and transfection*

FRTL5, FRTL5-KiMSV and FRTL5-KiMSV-HMGA1as cells (Berlingieri et al., 2002) were cultured in Coon's modified F12 medium supplemented with 5% of calf serum and six growth factors. FRO human anaplastic thyroid cancer cells were cultured in Dulbecco's modified Eagle's medium (DMEM) (Sigma) supplemented with 10% fetal bovine serum (FBS) (Invitrogen). MCF7 is a breast cancer cell line isolated from a 69-year-old

Caucasian woman (Soule et al., 1973). MCF7-HMGA1 and MCF7-EV are MCF7 cells transfected with a HMGA1 expression vector or the backbone vector, respectively (Baldassarre et al., 2003; Mansueto et al., 2010). They were cultured as described for the FRO cells.

MEFs from wild type (wt) and *Hmga1* null mice were obtained from 12.5-day-old embryos. Cells were cultured in DMEM (Sigma) supplemented with 10% fetal bovine serum (FBS) (Invitrogen) (Fedele et al., 2006a,b). For oligonucleotide transfection cells were transfected with 50 nmol/mL pre-miRNA precursor, inhibitor, or a control no-targeting scrambled oligonucleotides (Ambion, Austin, TX) using siPORT Neo-FX™ transfecting reagent (Ambion), according to the manufacturer's protocol.

For the transfection of the p-miRNA constructs, cells were transfected with 5 μg of the p-miRNA precursors expressing vectors carrying miR-10b and miR-603 or the backbone vector (SBI System Biosciences, Mountain View, CA), using Lipofectamine 2000 (Invitrogen), according to the manufacturer's instructions.

2.4. Chromatin immunoprecipitation assay

FRTL5-KiMSV cells were processed for ChIP experiments as reported (Pierantoni et al., 2006). The chromatin of FRTL5-KiMSV cells was cross-linked and immunoprecipitated with the specific HMGA1 (Pierantoni et al., 2001) and HMGA2 (Fedele et al., 2006a,b) antibodies. The sequence of the primers are described in Supplementary Material.

2.5. Plasmids and constructs

The 3′-UTR regions of *CCND1* and *CCND2*, including binding sites for miR-603 and the 3′-UTR region of *PTEN*, including binding sites for miR-10b, were amplified by PCR by using the primers described in Supplementary Material. The amplified fragments were cloned into pGL3-Control Firefly luciferase vector (Promega, Madison, WI, USA) at the *Xba*I site immediately downstream the stop codon of the luciferase gene. The Renilla luciferase vector (pRL-CMV) was purchased by Promega. Deletion of miR10b-binding site in the PTEN-3′-UTR was introduced by using QuikChange Site-directed Mutagenesis Kit (Stratagene) following the manufacturer's instructions. The primers used are reported in Supplementary Material. p-miRNA vectors expressing miR-10b and miR-603 under the transcriptional control of the CMV promoter were purchased from SBI System Biosciences.

2.6. Protein extraction, western blotting and antibodies

Western blot analyses were performed as previously described (Palmieri et al., 2012) and the membranes were incubated with antibodies against cyclin D1 (sc-F18, Santa Cruz), cyclin D2 (sc-181 Santa Cruz), PTEN (sc-7974, Santa Cruz) and γ-tubulin (sc-8035, Santa Cruz).

2.7. Luciferase target assay

For luciferase reporter experiments, FRTL5 cells were co-transfected using siPORT with the modified Firefly luciferase vector (200 ng), the Renilla luciferase reporter plasmid (pRL-CMV; Promega) (20 ng) and the miRNA oligonucleotideos (50 nmol/ml). Firefly and *Renilla* luciferase activities were measured 48 h after transfection with the Dual-Luciferase Reporter Assay System (Promega). Firefly activity was normalized to *Renilla* activity as control of transfection efficiency.

2.8. Growth curve assay

FRTL5 and FRO cells were plated in 24-well and transfected with 50 nmol/ml pre-miR miRNA precursor or scrambled oligonucleotide (Ambion), using siPORT neoFX. Cells were counted after 24, 48, 72 and 96 h.

2.9. Colony-forming assay

FRTL5 cells were transfected with 5 μg of miR-10b and miR-603 precursors (SBI System Biosciences) or the backbone vector, along with a construct expressing the neomycin-resistance gene. Transfected cells were selected by using 1 μg/ml neomycin diluted in the medium used for culture. After 15 days, cells were fixed and stained with 0.1% crystal violet in 20% methanol and colonies were counted.

2.10. Flow cytometry

After trypsinization, cells were washed once in phosphate-buffered saline and fixed in 70% ethanol overnight. Staining for DNA content was performed with 2 μg/ml propidium iodide and 20 μg/ml RNase A for 30 min. We used a FACScan flow cytometer (Becton Dickinson, San Jose, CA) that was interfaced with a Hewlett–Packard computer (Palo Alto, CA). Cell cycle results were analysed with the CELL-FIT program (Becton Dickinson).

2.11. Scratch wound healing assay

Cells were plated at equal density in six-well plates. After confluence, the cells were treated with mytomicin C for 3 h and wounds were generated with a sterile pipette. Then, cells were washed twice with PBS, and fresh culture medium was added. The wound areas were marked and the cultures were maintained in DMEM medium (including 10% FBS) at 37 °C in a humidified incubator with 5% CO_2. At different time points the migratory distance of the cells was assessed under an inverted phase-contrast microscope.

2.12. Soft agar colony assay

Cells were mixed in DMEM 2 (Sigma), tryptose phosphate buffer, and 1.25% of Noble Agar (Difco Laboratories Inc., Detroit, MI) and plated in 60-mm dishes on the top of 1% agar base. The colonies were counted after two weeks.

2.13. Statistical analysis

Student's *t*-test was used to determine the significance for all the quantitative experiments. All error bars represent the standard error (s.e.). Statistical significance, assessed for all the tests by calculating the *p*-value, was <0.05.

3. Results

3.1. *miRNA expression profile of normal and KiMSV-infected rat thyroid cells*

We analyzed a miRNACHIP microarray (Liu et al., 2004) to evaluate the miRNA expression profile of the FRTL5 (normal rat thyroid cell line), FRTL5-KiMSV (KiMSV-infected FRTL5 cells expressing the HMGA1 proteins) and FRTL5-KiMSV-HMGA1as (KiMSV-infected FRTL5 cells where the expression of HMGA1 has been silenced by antisense methodology). By applying the statistical analysis (see Materials and Methods), we obtained a list of differentially expressed miRNAs ($p < 0.05$) in the different cell lines analyzed. Thirty miRNAs were overexpressed with a fold-change equal or higher than two in the FRTL5-KiMSV (FRTL5-Ki) cells *versus* the normal rat thyroid cells (FRTL5). Conversely, eleven miRNAs showed an evident reduction in their expression in the KiMSV-transformed cells compared with the uninfected cells (Table 1). Among these genes regulated by cell transformation, there are miR-10b, miR-21, miR-125b, miR-221 and miR-222 that are positively and miR-34a and miR-603 that are negatively regulated, by HMGA1 expression. Indeed, their expression is drastically reduced or increased, respectively, in the FRTL5-KiMSV-HMGA1as with respect the FRTL5-KiMSV cells. Subsequently, we validated the results obtained by miRNACHIP array analysis by evaluating the expression of miR-10b, miR-21, miR-125b, miR- 221, miR-222, miR-603 and mir-34a by real-time PCR (Figure 1A).

Next, we investigated whether the dependency on HMGA1 expression of some miRNAs was restricted to the transformed thyroid cells or a more general event analyzing their expression in a breast cancer cell line, MCF7, transfected with HMGA1 (MCF7-HMGA1) (Baldassarre et al., 2003) and mouse embryonic fibroblasts (MEFs) null for *Hmga1* and relative wild-type (wt) counterparts (Fedele et al., 2006a, b). As shown in Figure 1B, miR-10b was much more expressed in MCF7-HMGA1 with respect to the MCF7 cells transfected with the empty vector, whereas it was downregulated in *Hmga1* null MEFs with respect to the wt ones. Conversely, miR-603 showed an opposite behavior being less expressed in MCF7-HMGA1 and wt MEFs in comparison with MCF7-empty vector and *Hmga1* null MEFs (Figure 1C). The expression of miR-21, miR-125b, miR-222 and miR-34a did not show significant differences in MCF7 expressing or not the HMGA1 proteins. Moreover, the expression of miR-21, miR-125b, miR-221 and miR-222 was, in contrast with the results observed in FRTL5 cells, higher in the *Hmga1* null MEFs than in the wt ones whereas no significant differences in miR-34a expression were observed in these cells (Supplementary Figure 1 in Supplementary Information). Therefore, we decided to focus on miR-10b and miR-603 since their expression was depending on HMGA1 in more than one cell system.

Table 1 – a) miRNAs upregulated in FRTL5-Ki vs FRTL5 cells. b) miRNAs downregulated in FRTL5-Ki vs FRTL 5 cells.

	FRTL5-Ki vs FRTL5[a]	FRTL5-Ki-HMGA1as vs FRTL5[a]	Unique id
a)			
1	5.697651549	0.208987416	miR-211
2	26.44651332	0.795418737	miR-221
3	5.264432083	0.573778937	miR-222
4	1.265228455	0.844394214	miR-135a
5	14.55630099	1.297759935	miR-10b
6	1.258664206	0.699995641	miR-125a-5p
7	9.464898863	6.260278691	miR-181c
8	7.105168512	0.368761397	miR-125b
9	4.896899836	4.368751686	miR-296-3p
10	2.358407465	1.868430445	miR-139-3p
11	2.826323567	1.129499769	miR-181a-2*
12	2.893767415	2.160719366	miR-136
13	1.785567148	0.960286886	miR-24
14	2.891293676	2.495793443	miR-30c-1*
15	1.996377498	0.321989938	miR-23a
16	4.512756223	1	miR-21
17	3.342764364	2.652455609	miR-99a
18	2.527050609	0.377153025	miR-25
19	7.384708811	3.386067312	miR-10a
20	1.454997404	1.068759859	miR-31
21	3.443864288	0.937230018	miR-29b
22	5.040132014	3.525231566	miR-345
23	1.213669855	0.298127602	miR-191*
24	3.744986798	1.212977885	miR-19a
25	2.145461955	1.350767822	miR-92a
26	2.984606791	2.113836493	miR-154
27	1.435303772	1.001108842	miR-219-2-3p
28	7.599428473	6.343859975	miR-548a-3p
29	5.583175923	0.512242463	miR-563
30	2.157043158	1.609210135	let-7e
b)			
1	0.417806325	0.457007065	miR-129-3p
2	0.584183688	0.816260924	miR-595
3	0.557292828	0.721803412	miR-191
4	0.67287794	1.121527038	miR-589
5	0.573515486	2.216145637	miR-583
6	0.718765203	0.929192034	miR-370
7	0.755058475	1.276243767	miR-766
8	0.475213322	0.576507942	miR-133b
9	0.644385477	1.000823991	miR-660
10	0.39080976	1.068527273	miR-603
11	0.312565682	0.354068984	miR-34a

Note:
* Signifies the miR Unique ID which is reported according with the conventional nomenclature of miRBAS (www.mirbase.org).
a The values indicate the fold-change compared with FRTL5 cells.

3.2. *HMGA1 protein binds to a region upstream of the miR-10b and miR-603 loci*

Next, we investigated whether HMGA1 directly binds to the regulatory regions of miR-10b and miR-603. We searched for regions rich in AT sequences since it is known that the HMGA proteins bind DNA in AT-rich regions through three basic domains called "AT-hooks" (Reeves and Nissen, 1990). Then, we found putative (AT-rich) HMGA-binding sequences in three regions located 2000 bp upstream the miR-10b and miR-603 genes. We performed chromatin immunoprecipitation (ChIP) assays to determine whether the HMGA proteins could bind to these sequences. To this aim, the chromatin of FRTL5-KiMSV cells was cross-linked and immunoprecipitated with anti-HMGA1 and anti-HMGA2 antibodies. Immunoprecipitated DNA was then analyzed by semiquantitative and quantitative PCR using primers covering the putative HMGA-binding sites.

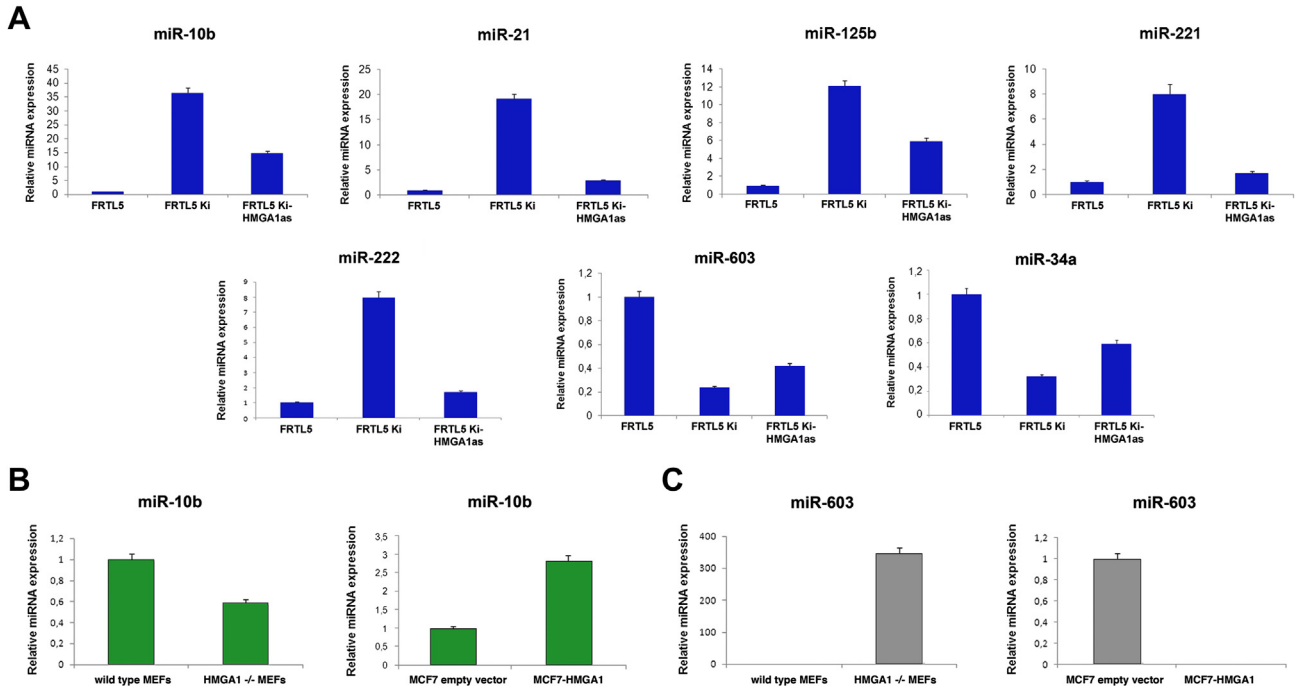

Figure 1 – (A) Validation of miRNA microarray data by qRT-PCR. qRT-PCR analysis of miR-10b, miR-21, miR-125b, miR-221, miR-222, miR-603 and miR-34a was carried out on FRTL5, FRTL5-KiMSV and FRTL5-KiMSV-HMGA1as. The expression values indicate the relative change in the expression levels between FRTL5 and FRTL5-KiMSV cells, assuming that the mean value of the FRTL5 cells was equal to 1. Each bar represents the mean value ± s.e. from three independent experiments performed in triplicate. miR-10b (B) and miR-603 (C) expression in wild type and *Hmga1*–/– MEFs and MCF7-EV and MCF7-HMGA1 cells. The relative expression values indicate the relative change in the expression levels between *Hmga1*–/– and wt MEFs, MCF7-HMGA1 and MCF7-EV samples, assuming that the mean value of the wt MEFs and MCF7-EV cells samples was equal to 1. Each bar represents the mean value ± s.e. from three independent experiments performed in triplicate.

Amplification of all the three analysed sequences upstream the miR-10b gene was observed in chromatin from FRTL5-KiMSV, immunoprecipitated with anti HMGA1 and HMGA2 antibodies, while we observed amplification only in two out of the three analysed sequences upstream the miR-603. No amplification was observed with anti-IgG precipitates, used as negative control (Figure 2), which shows that the binding is specific for the region upstream of the miR-10b and miR-603. Therefore, these

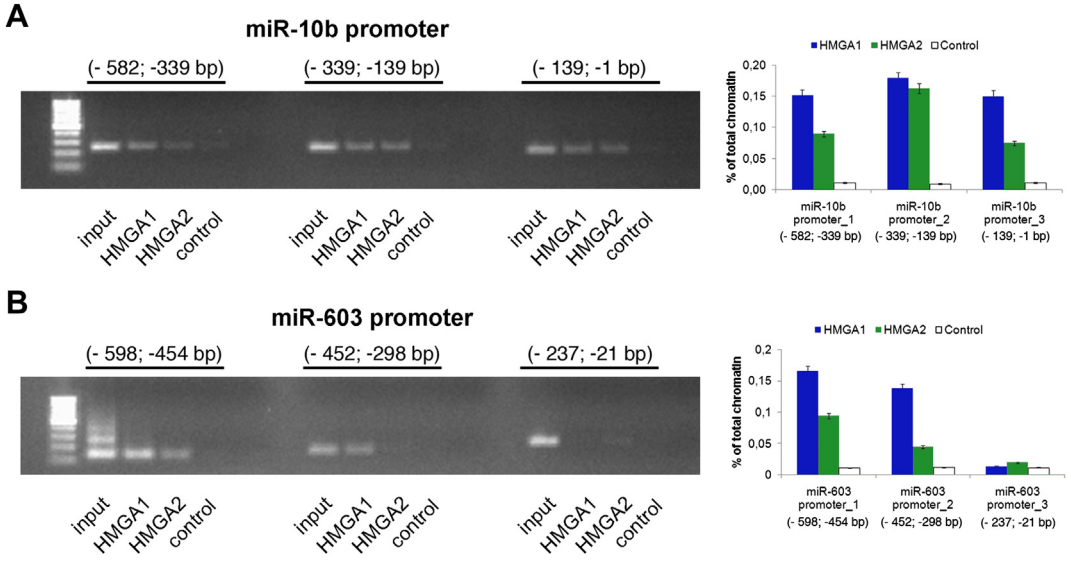

Figure 2 – HMGA1 and HMGA2 bind the regions upstream miR-10b and miR-603. (A–B) The chromatin of FRTL5-KiMSV cells was immunoprecipitated with anti-HMGA1 and anti-HMGA2 antibodies. Input and immunoprecipitated DNA were analyzed by semiquantitative PCR (left panel) or qPCR (right panel) using specific primers covering the indicated miR-10b and miR-603 upstream regions. Normal rabbit IgGs were used as negative control. Error bars indicate confidence intervals of three independent experiments performed in triplicate.

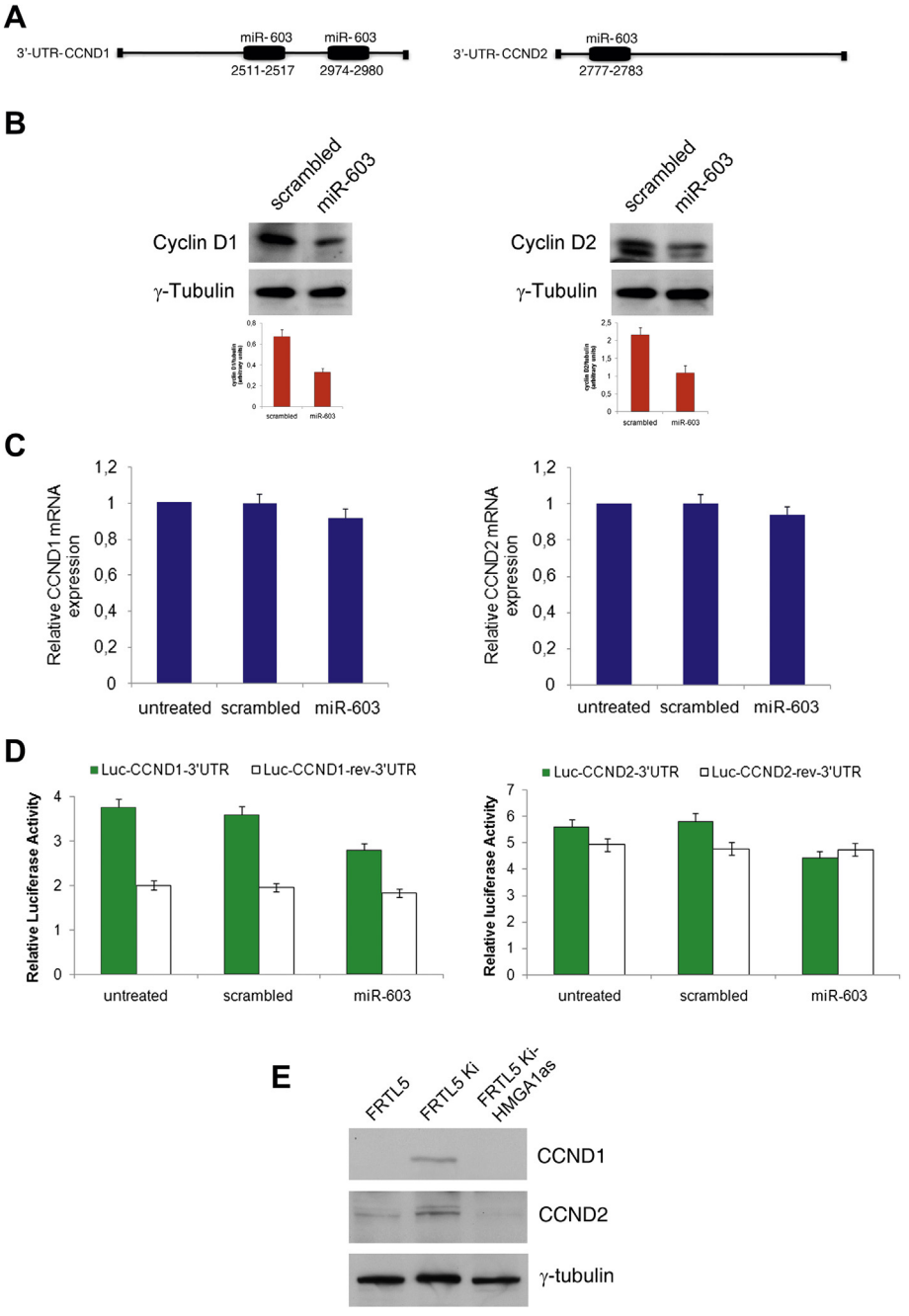

Figure 3 – miR-603 targets CCND1 and CCND2. (A) Schematic representation of the 3′-UTR sites of the *CCND1* and *CCND2* gene targeted by miR-603. (B) Western blot analysis of cyclin D1 (left panel) and cyclin D2 (right panel) protein levels in FRTL5 cells transfected with miR-603 and a scrambled oligonucleotide. γ-tubulin expression was analyzed as loading control. The densitometric analysis was performed using ImageJ software and normalizing to the γ-tubulin. (C) qRT–PCR analysis of *CCND1* (left panel) and *CCND2* (right panel) mRNA. Relative expression values indicate the relative change in *CCND1* and *CCND2* mRNA expression levels between miR-treated or untreated compared with scrambled oligonucleotide-treated cells, normalized with G6PD, assuming that value of the scrambled oligonucleotide-treated samples was equal to 1. Each bar represents the mean value ± s.e. from three independent experiments performed in triplicate. (D) Relative luciferase activity in FRTL5 cells transiently transfected with Luc-CCND1-3′UTR (left panel) or Luc-CCND2-3′UTR (right panel) either in sense or antisense orientation along with the indicated miRNA oligonucleotide or untreated cells compared with a scrambled oligonucleotide. The relative activity of firefly luciferase expression was standardized to a transfection control, using *Renilla* luciferase. The scale bars represent the mean ± s.e. of three independent experiments performed in triplicate. (E) Western blot analysis of Cyclin D1 and Cyclin D2 protein levels in FRTL5, FRTL5-KiMSV and FRTL5-KiMSV-HMGA1as cells. γ-tubulin expression was analyzed as loading control.

results indicate that the HMGA1 and HMGA2 proteins are able to bind *in vivo* a region located upstream the miR-10b and miR-603 that has likely regulatory functions.

3.3. CCND1 and CCND2 are targets of miR-603

Since miRNAs are capable to modulate gene expression by targeting mRNA, we used bioinformatic tools (Target Scan, mirGen and miRanda) to search for mRNA targets of miR-603. We found several predicted targets involved in many different biological processes, but we focused our attention on *CCND1* (cyclin D1) which has been mentioned as a key gene in cell cycle control and it is frequently overexpressed in cancer cells, contributing to cell proliferation and migration (Li et al., 2006), and *CCND2* (cyclin D2) which has a very important role in G1/S transition of the cell cycle (Sicinski et al., 1996). The sites that match the miR-603 seed sequence were predicted in both 3′-UTR sequences of these genes (Figure 3A). To validate the influence of miR-603 on these targets, we transfected the miR-603 oligonucleotide precursor into FRTL5 cells and we searched for changes in cyclin D1 and D2 protein levels by western blot analysis. After the transfection of miR-603, we found an evident reduction in cyclin D1 and D2 protein levels as compared with the scrambled oligonucleotide (Figure 3B). No changes in *CCND1* and *CCND2* mRNA levels were detected after transfection with miR-603 in comparison with the scrambled oligonucleotide or untransfected cells (Figure 3C). This result validates a post-transcriptional regulation of cyclin D1 and D2 proteins by miR-603, and excludes its role in *CCND1* and *CCND2* mRNA degradation.

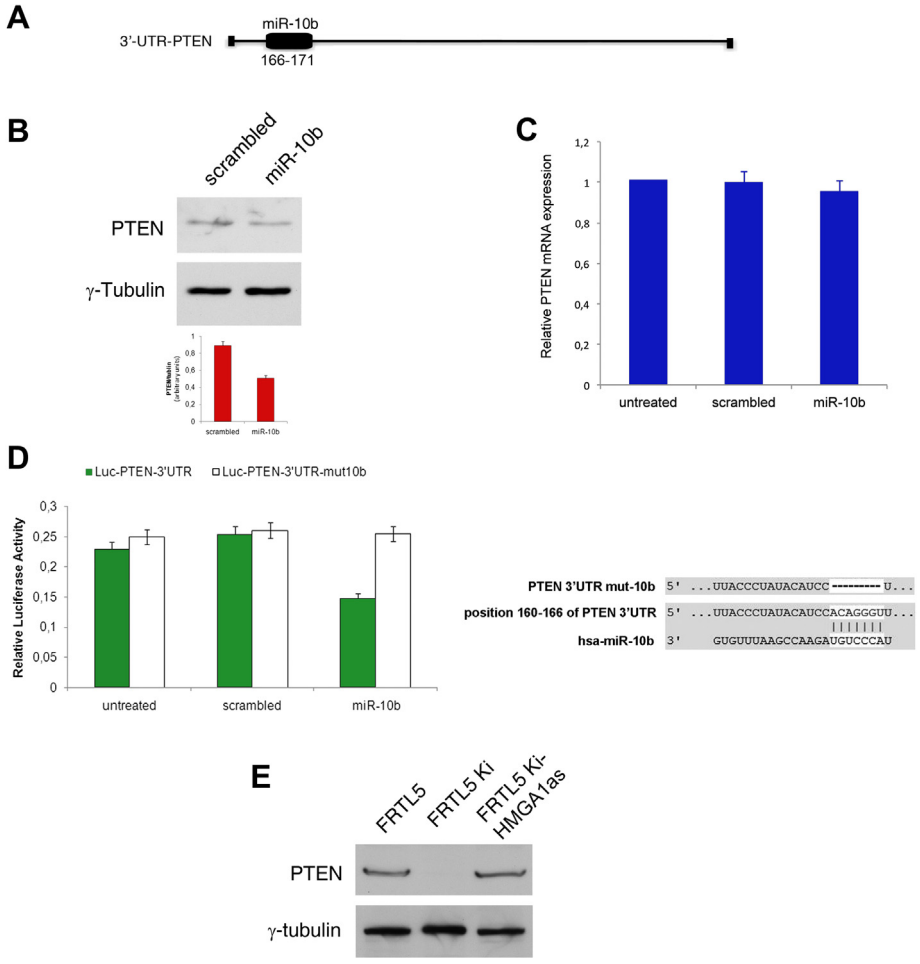

Figure 4 – miR-10b targets PTEN. (A) Schematic representation of the 3′-UTR site of the *PTEN* gene targeted by miR-10b. (B) Western blots of the PTEN protein expression in FRTL5 cells transfected with miR-10b or a scrambled oligonucleotide. γ-tubulin expression was analyzed as loading control. The densitometric analysis was performed using ImageJ software and normalizing to γ-tubulin. (C) qRT-PCR analysis of *PTEN* mRNA. Relative expression values indicate the relative change in *PTEN* mRNA expression levels between miRNA-treated or untreated cells compared with the scrambled oligonucleotide-treated ones, normalized with G6PD, assuming that value of the scrambled oligonucleotide-treated sample was equal to 1. Each bar represents the mean value ± s.e. from three independent experiments performed in triplicate. (D) Relative luciferase activity in FRTL5 cells transiently transfected with Luc-PTEN-3′UTR or with Luc-PTEN-3′UTR-mut10b along with miR-10b oligonucleotide or untransfected in comparision with a scrambled oligonucleotide. The relative activity of firefly luciferase expression was standardized to a transfection control, using *Renilla* luciferase. The scale bars represent the mean ± s.e. of three independent experiments performed in triplicate. The right panel shows the 3′-UTR site of the *PTEN* gene targeted by miR-10b, the miR-10b seed sequence and the 3′-UTR site of the *PTEN* gene carrying a deletion in the miR-10b recognition site. (E) Western blot analysis of PTEN protein levels in FRTL5, FRTL5-KiMSV and FRTL5-KiMSV-HMGA1as cells. γ-tubulin expression was analyzed as loading control.

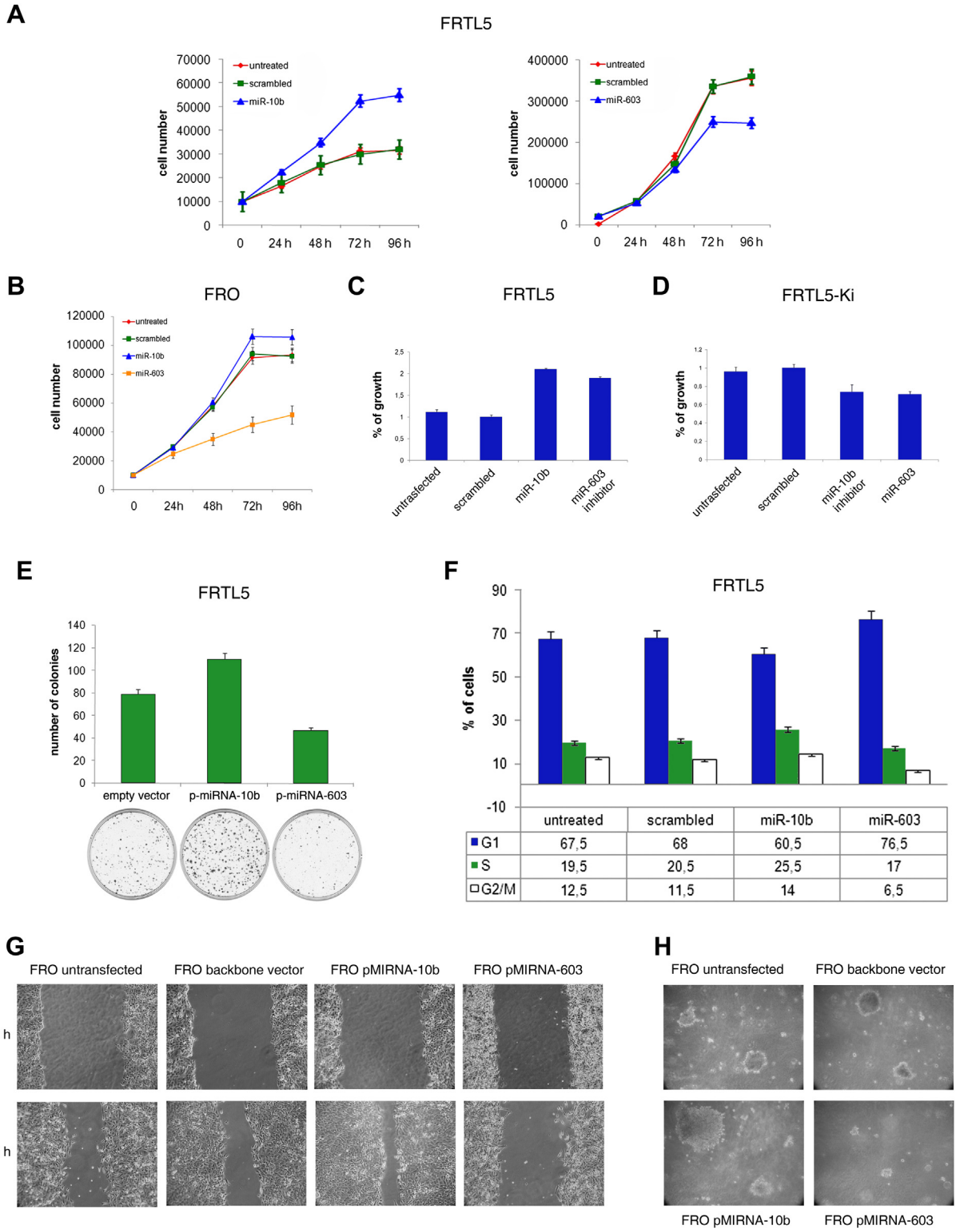

Figure 5 – miR-10B and miR-603 effects on cell proliferation and migration. (A) Cell growth curves of FRTL5 cells transfected with miR-10b (left panel) and miR-603 (right panel) compared with the untransfected or scrambled oligonucleotide-transfected cells. The cells were seeded in 24-well plates at 1 × 10^4 cells/well. The cells were counted each 24 h for 96 h after plating. *Y*-axis represents absolute viable cell count. The mean values ± s.e. derive from three independent experiments performed in triplicate. (B) Cell growth curve of FRO cells transfected with miR-10b and miR-603 in comparison with the untransfected or scrambled oligonucleotide-transfected cells. The mean values ± s.e. derive from three independent experiments performed in triplicate. (C–D) Cell growth assays on FRTL5 and FRTL5-KiMSV cells: untransfected or transfected FRTL5 cells with miR-10b precursor, miR-603 inhibitor or a scrambled oligonucleotide (C), and untransfected or transfected FRTL5-KiMSV cells with miR-10b inhibitor, miR-603 precursor or a scrambled oligonucleotide. (D) The cells were seeded in 24-well plates at 1 × 10^4 cells/well

To demonstrate that the direct interaction between the analyzed miRNAs and the *CCND1* and *CCND2* mRNAs was responsible for protein level decrease, we inserted the 3′-UTR of *CCND1* and *CCND2*, including the miR-603 seed sites, downstream the luciferase ORF, either in sense (Luc-CCND1-3′UTR and Luc-CCND2-3′UTR) or in antisense (Luc-CCND1rev-3′UTR and Luc-CCND2rev-3′UTR) orientation. The luciferase activity of the Luc-sense-3′UTR constructs was markedly diminished after transfection of miR-603, compared with the scrambled oligonucleotide-transfected or untransfected cells, while the luciferase activity of Luc-antisense-3′UTR constructs did not change, indicating that the reduction of cyclin D1 and D2 protein expression by miR-603 was dependent on their direct binding to its 3′-UTR (Figure 3D).

Consistently with the ability of miR-603 to target *CCND1* and *CCND2*, the levels of the proteins coded for by these genes are inversely correlated with miR-603 expression in FRTL5, FRTL5-KiMSV and FRTL5-KiMSV-HMGA1as (Figure 3E).

3.4. *miR-10b targets PTEN*

Bioinformatic analysis predicted also for miR-10b several targets, some of them already validated in previous studies (Jo et al., 2011; Kim et al., 2011; Liu et al., 2012). Among the predicted target genes we focused on the PTEN gene. Indeed, PTEN is an important tumor suppressor, whose expression is frequently altered in a wide spectrum of human cancers (Hollander et al., 2011) including thyroid malignancies (Bruni et al., 2000). Moreover, recent findings demonstrate that subtle changes in PTEN expression levels dictate critical outcomes in tumor initiation and progression *in vivo* (Alimonti et al., 2010; Berger et al., 2011; Trotman et al., 2003). The sites that match the miR-10b seed sequence were predicted in the 3′-UTR sequence of this gene (Figure 4A). To validate the influence of miR-10b on PTEN protein expression, we transfected miR-10b oligonucleotide precursor in FRTL5 cells and searched for changes in PTEN protein levels by western blot analysis. The introduction of miR-10b into FRTL5 cells decreased PTEN protein levels as compared to the scrambled oligonucleotide-transfected cells (Figure 4B). The analysis of the *PTEN* specific mRNA levels after transfection with miR-10b did not show significant changes in comparison with the scrambled oligonucleotide-transfected or untransfected FRTL5 cells indicating that miR-10b regulates PTEN protein levels acting at post-transcriptional level (Figure 4C). Finally, to demonstrate that the direct interaction between the miR-10b and the *PTEN* mRNA was responsible for the decrease in PTEN protein levels, we inserted the 3′-UTR of PTEN, including the miR-10b seed sites, downstream of the luciferase ORF. The luciferase activity, measured after 48h, was significantly reduced after transfection with miR-10b compared with scrambled oligonucleotide transfected- or untransfected cells, indicating that the reduction of PTEN protein expression by miR-10b was dependent on its direct binding to its 3′-UTR. Conversely, no effect was observed by miR-10b on the luciferase activity when we assayed a reporter vector carrying a deletion in the seed sequence for miR-10b (Figure 4D).

Consistently with the ability of miR-10b to target PTEN, the levels of this protein are inversely correlated with miR-10b expression in FRTL5, FRTL5-KiMSV and FRTL5-KiMSV-HMGA1as (Figure 4E).

3.5. *miR-10b and miR-603 expression affects cell proliferation in opposite ways*

To understand the role of the miR-10b and miR-603 in thyroid cell transformation we analyzed their effects on cell proliferation. Therefore, we performed a growth curve assay on FRTL5 cells untransfected or transiently transfected with miR-10b, miR-603, or a scrambled oligonucleotide. As shown in Figure 5A, a clear reduction in cell number was observed at 72 and 96 h after transfection with miR-603 compared with the control cells. Conversely, a significantly increased cell number was observed after transfection of miR-10b with respect to the scrambled oligonucleotide-transfected cells. Similar results were observed when human anaplastic thyroid carcinoma cells, FRO, were transfected with the same miRNAs (Figure 5B). Subsequently, we transfected the FRTL5 cells, which express low levels of miR-10b and high levels of miR-603, with the miR-10b oligonucleotide precursor and miR-603 inhibitor. In both the cases we observed an increased growth rate of the transfected cells, compared with that of the untransfected or scrambled oligonucleotide-transfected cells (Figure 5C). Conversely, when we transfected the FRTL5-KiMSV cells, which express high levels of miR-10b and low levels of miR-603, with the miR-10b inhibitor and miR-603 precursor, we observed a reduction of the growth rate (Figure 5D) with respect to the scrambled oligonucleotide-transfected cells.

Then, we carried out a colony-forming assay on FRTL5 cells after transfection with p-miRNA-expression vectors carrying miR-10b and miR-603 precursors, or with the backbone vector, along with a construct expressing the gene for the resistance to neomycin. As shown in Figure 5E, consistently with the results of the growth curve assay, the cells transfected with miR-10b-expression vector generated a higher number of colonies, whereas a lower number of colonies was produced by the cells transfected with miR-603 in comparison with the same cells transfected with the backbone vector.

and counted 96 h after plating. The reported results are the mean ± s.e. of three experiments compared to scrambled oligonucleotide-transfected cells. (E) Colony-forming assay performed on FRTL5 cells transfected with vectors expressing miR-10b or miR-603 or the empty vector. (F) Flow cytometric analysis of FRTL5 cells transfected with miR-10b and miR-603 or the scrambled oligonucleotide. Each bar represents the mean value ± s.e. of three independent experiments performed in triplicate. The percentage of cells in each phase is reported in the Table below. (G) Scratch wound migration assay of FRO cells untransfected or stably transfected with p-miR-10b, p-miR-603 or the backbone vector. The cells were plated at equal density in six-well plates and grown to confluence. Uniform scratch was made in each confluent layer culture, the extent of wound closure was monitored under a phase-contrast microscope, and photographs were taken at 0 and 15 h. (H) Soft agar colony assay of FRO cells untransfected or stably transfected with p-miR-10b, p-miR-603 or the backbone vector. 1×10^5 cells were plated in 60-mm dishes on the top of 1% agar base. The colonies were counted after 2 weeks. Representative colonies are shown.

Finally, to better characterize the effects of the analyzed miRNAs on cell cycle progression, FRTL5 cells were transfected with miRNA precursors or the scrambled oligonucleotide, and then analyzed by flow cytometry. As shown in Figure 5F, miR-10b-transfected cells displayed a decrease in the G1-phase population and an increase in the S-phase, compared with the scrambled oligonucleotide-transfected or untransfected cells, while miR-603-transfected cells displayed an increase in the G1-phase population and a decrease in the S-phase. These results indicate that the overexpression of these miRNAs affects the G1-S transition of the cell cycle progression in opposite ways.

3.6. *miR-10b and miR-603 expression affects cell migration and invasiveness*

To assess the role of miR-10b and miR-603 on cell migration we performed a scratch wound migration assay, which was carried out in FRO cells stably transfected with p-miR-10b and p-miR-603. The cells were incubated for 3 h with mitomycin-C to inhibit cell proliferation. The cell motility was monitored under a microscope at different time points after generation of the wound. As shown in Figure 5G, the closure of the wound was observed within 15 h in the FRO p-miR-10b cells, whereas the cells transfected with the backbone vector showed the wound closure after 20 h. Conversely, the closure of the wound occurred only after 24 h in the FRO p-miR-603 cells.

Furthermore, to investigate the role of miR-10b and miR-603 in the expression on the malignant phenotype we performing a soft agar assay. As shown in Figure 5H, the number of colonies shown by the FRO-miR-603 is lower with respect to the untransfected FRO cells or carrying the empty vector, whereas the FRO cells expressing the miR-10b show a number of colonies quite similar to the FRO-EV cells. However, the size of the colonies induced by the FRO-miR-10b cells is larger with respect to the size shown by the FRO cells untransfected or transfected with the backbone vector. Conversely, the FRO-miR-603 cells showed a smaller size.

Therefore, these results demonstrate that miR-603 reduces the migration and invasiveness of thyroid cancer cells while miR-10b has an opposite effect.

4. Discussion

HMGA1 and HMGA2 protein overexpression is a feature of malignant neoplasias playing a casual role in cell transformation modulating the transcription of a number of genes that have a critical role in the progression step of carcinogenesis. Both HMGA1 and HMGA2 exert their oncogenic activity through several mechanisms: induction of E2F1 (Fedele et al., 2006a,b) and AP-1 activity (Vallone et al., 1997), induction of cyclin A expression (Tessari et al., 2003), inactivation of p53-induced apoptosis (Frasca et al., 2006; Pierantoni et al., 2006), enhancement of the expression of proteins involved in inflammation (Baron et al., 2010; Resar, 2010), and modulation of genes involved in epithelial–mesenchymal transition (Tan et al., 2012; Wu et al., 2011). Since miRNAs have recently emerged as important regulators of gene expression and several studies demonstrate that the deregulation of their expression is involved in the process of carcinogenesis, we aimed at the identification of the miRNAs whose expression is dependent on the HMGA1 expression and, then, the definition of their role in cell transformation. For this purpose we could take advantage of the availability in our laboratory of an epithelial (representing the cell type from have origin the large majority of human malignant neoplasias) cell system where the malignant transformation is inhibited by the suppression of the HMGA expression by antisense methodology. Therefore, we analyzed the miRNA expression profile of normal thyroid cells and the same cells transformed by the v-*ras-Ki* oncogene transfected or not with an antisense *HMGA1* construct. The analysis of this experiment revealed the presence of several miRNAs whose expression depended on the expression of *v-ras-Ki* oncogene. Among these miRNAs, seven were modulated were by the expression of the HMGA1 proteins. It is noteworthy that among the miRNAs overexpressed in the *v-ras-Ki*-transformed cells we found miR-221 and miR-21 that have been described as upregulated in several human carcinomas (Garofalo et al., 2012; Volinia et al., 2006). Then, among the HMGA1-dependent miRNAs we decided to focus on the miR-10b and 603 since we found that their expression was dependent on HMGA1 expression also in wild type and *Hmga1* null MEFs, and breast carcinoma cells, MCF7, overexpressing or not HMGA1. We, first, demonstrated that the regulation of miR-10b and miR-603 by the HMGA1 proteins is direct, because the ChIP revealed that HMGA1 is able to bind a region upstream these miRNAs. Then, we identified the targets of these miRNAs: *CCND1* and *CCND2* were the targets of miR-603 and *PTEN* target of miR-10b. Indeed, these miRs have a matched sequence in the 3′-UTR sequences of the identified target genes, and their enforced expression decreases levels of the proteins encoded by the target genes. This effect seems due to an inhibition of the translation process since no significant changes are observed in the *CCND1* and *CCND2* and *PTEN* mRNA levels after miR-603 and miR-10b treatment. The regulation of PTEN and cyclin D1/2 proteins by these miRNAs certainly account for a role of miR-10b and miR-603 dysregulation in cell transformation. Indeed, PTEN has been identified as a tumour suppressor gene that is mutated in a large number of cancers at high frequency (Li et al., 1997; Liaw et al., 1997). *CCND1* and *CCND2* code for proteins belonging to the highly conserved cyclin family that function as regulatory subunits of CDK4 and CDK6, whose activity is required for cell cycle G1/S transition that is frequently altered in cancer (Li et al., 2006; Sicinski et al., 1996). Functional studies support the role of the regulation of these mRNAs in cell transformation. Indeed, enforced expression of miR-10b promotes cell proliferation with a decreased cell population in the G1 phase of the cell cycle and enhances cell migration. Conversely, an opposite effect is achieved when miR-603 is transfected.

Therefore, this study provides a novel mechanism by which HMGA1 contributes to malignant cell transformation, and suggests different approaches to a cancer therapy based on the block of the HMGA1 protein function. Indeed, this would be possible by: a) directly acting on these proteins; or b) increasing the level of the miRNAs that have HMGA1 as target (D'Angelo et al., 2012; Palmieri et al., 2012) or c) modifying the misexpression of the miRNAs that are modulated by HMGA1.

Conflict of interest

The authors declare no conflict of interest.

Acknowledgment

This work was supported by grants from Associazione Italiana per la Ricerca sul Cancro (AIRC) (IG 5346) and the Ministero dell'Università e della Ricerca Scientifica e Tecnologica – MIUR (PRIN 2008).

P. Mussnich is recipient of a fellowship from CAPES Foundation, Ministry of Education of Brazil (n°1956-10-8).

D. D'Angelo is recipient of a fellowship from Fondazione Italiana per la Ricerca sul Cancro (FIRC).

We thank Mario Berardone for the art-work.

Appendix A. Supplementary data

Supplementary data related to this article can be found at http://dx.doi.org/10.1016/j.molonc.2013.01.002.

REFERENCES

Abdulkadir, S.A., Krishna, S., Thanos, D., Maniatis, T., Strominger, J.L., Ono, S.J., 1995. Functional roles of the transcription factor Oct-2A and the high mobility group protein I/Y in HLA-DRA gene expression. J. Exp. Med. 182, 487–500.

Alimonti, A., Carracedo, A., Clohessy, J.G., Trotman, L.C., Nardella, C., Egia, A., Salmena, L., Sampieri, K., Haveman, W.J., Brogi, E., Richardson, A.L., Zhang, J., Pandolfi, P.P., 2010. Subtle variations in Pten dose determine cancer susceptibility. Nat. Genet. 42, 454–458.

Arlotta, P., Tai, A.K., Manfioletti, G., Clifford, C., Jay, G., Ono, S.J., 2000. Transgenic mice expressing a truncated form of the high mobility group I-C protein develop adiposity and an abnormally high prevalence of lipomas. J. Biol. Chem. 275, 14394–14400.

Baldassarre, G., Fedele, M., Battista, S., Vecchione, A., Klein-Szanto, A., Santoro, M., Waldmann, T.A., Azimi, N., Croce, C.M., Fusco, A., 2001. Onset of natural killer cell lymphomas in transgenic mice carrying a truncated HMGI-C gene by the chronic stimulation of the IL-2 and IL-15 pathway. Proc. Natl. Acad. Sci. USA 98, 7970–7975.

Baldassarre, G., Battista, S., Belletti, B., Thakur, S., Pentimalli, F., Trapasso, F., Fedele, M., Pierantoni, G., Croce, C.M., Fusco, A., 2003. Negative regulation of BRCA1 gene expression by HMGA1 proteins accounts for the reduced BRCA1 protein levels in sporadic breast carcinoma. Mol. Cell. Biol. 23 (7), 2225–2238.

Baron, R.M., Lopez-Guzman, S., Riascos, D.F., Macias, A.A., Layne, M.D., Cheng, G., Harris, C., Chung, S.W., Reeves, R., von Andrian, U.H., Perrella, M.A., 2010. Distamycin A inhibits HMGA1-binding to the P-selectin promoter and attenuates lung and liver inflammation during murine endotoxemia. PLoS One 14;5 (5), e10656.

Bartel, D.P., 2004. MicroRNAs: genomics, biogenesis, mechanism, and function. Cell 116, 281–297.

Berger, A.H., Knudson, A.G., Pandolfi, P.P., 2011. A continuum model for tumor suppression. Nature 476, 163–169.

Berlingieri, M.T., Manfioletti, G., Santoro, M., Bandiera, A., Visconti, R., Giancotti, V., Fusco, A., 1995. Inhibition of hmgi-c protein synthesis suppresses retrovirally induced neoplastic transformation of rat thyroid cells. Mol. Cell. Biol. 15, 1545–1553.

Berlingieri, M.T., Pierantoni, G.M., Giancotti, V., Santoro, M., Fusco, A., 2002. Thyroid cell transformation requires the expression of the HMGA1 proteins. Oncogene 21, 2971–2980.

Bruni, P., Boccia, A., Baldassarre, G., Trapasso, F., Santoro, M., Chiappetta, G., Fusco, A., Viglietto, G., 2000. PTEN expression is reduced in a subset of sporadic thyroid carcinomas: evidence that PTEN-growth suppressing activity in thyroid cancer cells mediated by p27kip1. Oncogene 19 (28), 3146–3155.

D'Angelo, D., Palmieri, D., Mussnich, P., Roche, M., Wierinckx, A., Raverot, G., Fedele, M., Croce, C.M., Trouillas, J., Fusco, A., 2012. Altered MicroRNA expression profile in human pituitary GH adenomas: down-regulation of miRNA targeting HMGA1, HMGA2, and E2F1. J. Clin. Endocrinol. Metab. 97, E1128–E1138.

Fabbri, M., Croce, C.M., Calin, G.A., 2008. MicroRNAs. Cancer J. 14, 1–6.

Fedele, M., Battista, S., Kenyon, L., Baldassarre, G., Fidanza, V., Klein-Szanto, A.J., Parlow, A.F., Visone, R., Pierantoni, G.M., Outwater, E., Santoro, M., Croce, C.M., Fusco, A., 2002. Overexpression of the HMGA2 gene in transgenic mice leads to the onset of pituitary adenomas. Oncogene 21, 3190–3198.

Fedele, M., Pentimalli, F., Baldassarre, G., Battista, S., Klein-Szanto, A.J.P., Kenyon, L., Visone, R., De Martino, I., Ciarmiello, A., Arra, C., Viglietto, G., Croce, C.M., Fusco, A., 2005. Transgenic mice overexpressing the wild-type form of the HMGA1 gene develop mixed growth hormone/prolactin cell pituitary adenomas and natural killer cell lymphomas. Oncogene 24, 3427–3435.

Fedele, M., Fidanza, V., Battista, S., Pentimalli, F., Klein-Szanto, A.J., Visone, R., De Martino, I., Curcio, A., Morisco, C., Del Vecchio, L., Baldassarre, G., Arra, C., Viglietto, G., Indolfi, C., Croce, C.M., Fusco, A., 2006a. Haploinsufficiency of the Hmga1 gene causes cardiac hypertrophy and myelo-lymphoproliferative disorders in mice. Cancer Res. 66 (5), 2536–2543.

Fedele, M., Visone, R., De Martino, I., Troncone, G., Palmieri, D., Battista, S., Ciarmiello, A., Pallante, P., Arra, C., Melillo, R.M., Helin, K., Croce, C.M., Fusco, A., 2006b. HMGA2 induces pituitary tumorigenesis by enhancing E2F1 activity. Cancer Cell 9, 459–471.

Fedele, M., Fusco, A., 2010. HMGA and Cancer. Biochim. Biophys. Acta 1799, 48–54.

Fedele, M., Visone, R., De Martino, I., Palmieri, D., Valentino, T., Esposito, F., Klein-Szanto, A., Arra, C., Ciarmiello, A., Croce, C.M., Fusco, A., 2011. Expression of a truncated Hmga1b gene induces gigantism, lipomatosis and B-cell lymphomas in mice. Eur. J. Cancer 47, 470–478.

Frasca, F., Rustighi, A., Malaguarnera, R., Altamura, S., Vigneri, P., Del Sal, G., Giancotti, V., Pezzino, V., Vigneri, R., Manfioletti, G., 2006. HMGA1 inhibits the function of p53 family members in thyroid cancer cells. Cancer Res. 66, 2980–2989.

Fusco, A., Berlingieri, M.T., Di Fiore, P.P., Portella, G., Grieco, M., Vecchio, G., 1987. One- and two-step transformations of rat thyroid epithelial cells by retroviral oncogenes. Mol. Cell. Biol. 7 (9), 3365–3370.

Fusco, A., Fedele, M., 2007. Roles of HMGA proteins in cancer. Nat. Rev. Can. 7, 899–910.

Garofalo, M., Quintavalle, C., Romano, G., Croce, C.M., Condorelli, G., 2012. miR221/222 in cancer: their role in tumor progression and response to therapy. Curr. Mol. Med. 12, 27–33.

Giancotti, V., Pani, B., D'Andrea, P., Berlingieri, M.T., Di Fiore, P.P., Fusco, A., Vecchio, G., Philp, R., Crane-Robinson, C., Nicolas, R.H., 1987. Elevated levels of a specific class of nuclear

phosphoproteins in cells transformed with v-ras and v-mos oncogenes and by cotransfection with c-myc and polyoma middle T genes. EMBO J. 6 (7), 1981–1987.
Hollander, M.C., Blumenthal, G.M., Dennis, P.A., 2011. PTEN loss in the continuum of common cancers, rare syndromes and mouse models. Nat. Rev. Can. 11, 289–301.
Jo, D.H., Kim, J.H., Park, W.Y., Kim, K.W., Yu, Y.S., Kim, J.H., 2011. Differential profiles of microRNAs in retinoblastoma cell lines of different proliferation and adherence patterns. J. Pediatr. Hematol. Oncol. 33, 529–533.
Kim, K., Lee, H.C., Park, J.L., Kim, M., Kim, S.Y., Noh, S.M., Song, K.S., Kim, J.C., Kim, Y.S., 2011. Epigenetic regulation of microRNA-10b and targeting of oncogenic MAPRE1 in gastric cancer. Epigenetics 6, 740–751.
Lehming, N., Thanos, D., Brickman, J.M., Ma, J., Maniatis, T., Ptashne, M., 1994. An HMG-like protein that can switch a transcriptional activator to a repressor. Nature 371, 175–179.
Li, J., Yen, C., Liaw, D., Podsypanina, K., Bose, S., Wang, S.I., Puc, J., Miliaresis, C., Rodgers, L., McCombie, R., Bigner, S.H., Giovanella, B.C., Ittmann, M., Tycko, B., Hibshoosh, H., Wigler, M.H., Parsons, R., 1997. PTEN, a putative protein tyrosine phosphatase gene mutated in human brain, breast, and prostate cancer. Science 275, 1943–1947.
Li, Z., Wang, C., Prendergast, G.C., Pestell, R.G., 2006. Cyclin D1 functions in cell migration. Cell Cycle 5, 2440–2442.
Liau, S.S., Jazag, A., Ito, K., Whang, E.E., 2007. Overexpression of HMGA1 promotes anoikis resistance and constitutive Akt activation in pancreatic adenocarcinoma cells. Br. J. Cancer 96, 993–1000.
Liaw, D., Marsh, D.J., Li, J., Dahia, P.L., Wang, S.I., Zheng, Z., Bose, S., Call, K.M., Tsou, H.C., Peacocke, M., Eng, C., Parsons, R., 1997. Germline mutations of the PTEN gene in Cowden disease, an inherited breast and thyroid cancer syndrome. Nat. Genet. 16, 64–67.
Liu, C.G., Calin, G.A., Meloon, B., Gamliel, N., Sevignani, C., Ferracin, M., Dumitru, C.D., Shimizu, M., Zupo, S., Dono, M., Alder, H., Bullrich, F., Negrini, M., Croce, C.M., 2004. An oligonucleotide microchip for genome-wide microRNA profiling in human and mouse tissues. Proc. Natl. Acad. Sci. USA 101, 9740–9744.
Liu, Z., Zhu, J., Cao, H., Ren, H., Fang, X., 2012. miR-10b promotes cell invasion through RhoC-AKT signaling pathway by targeting HOXD10 in gastric cancer. Int. J. Oncol. 40, 1553–1560.
Livak, K.J., Schmittgen, T.D., 2001. Analysis of relative gene expression data using real-time quantitative PCR and $2^{-\Delta\Delta CT}$ method. Methods 25, 402–408.
Mansueto, G., Forzati, F., Ferraro, A., Pallante, P., Bianco, M., Esposito, F., Iaccarino, A., Troncone, G., Fusco, A., 2010. Identification of a new pathway for tumor progression: MicroRNA-181b Up-regulation and CBX7 down-regulation by HMGA1 protein. Genes Cancer 1 (3), 210–224.
Miska, E.A., 2005. How microRNAs control cell division, differentiation and death. Curr. Opin. Genet. Dev. 15, 563–568.
Palmieri, D., D'Angelo, D., Valentino, T., De Martino, I., Ferraro, A., Wierinckx, A., Fedele, M., Trouillas, J., Fusco, A., 2012. Downregulation of HMGA-targeting microRNAs has a critical role in human pituitary tumorigenesis. Oncogene 31, 3857–3865.
Pierantoni, G.M., Fedele, M., Pentimalli, F., Benvenuto, G., Pero, R., Viglietto, G., Santoro, M., Chiariotti, L., Fusco, A., 2001. High mobility group I (Y) proteins bind HIPK2, a serine- threonine kinase protein which inhibits cell growth. Oncogene 20, 6132–6141.
Pierantoni, G.M., Rinaldo, C., Esposito, F., Mottolese, M., Soddu, S., Fusco, A., 2006. High mobility group A1 (HMGA1) proteins interact with p53 and inhibit its apoptotic activity. Cell. Death Differ. 13, 1554–1563.
Reeves, R., Nissen, M.S., 1990. The AT DNA-binding domain of mammalian high mobility group I chromosomal proteins. A novel peptide motif for recognizing DNA structure. J. Biol. Chem. 265, 8573–8582.
Resar, L.M., 2010. The high mobility group A1 gene: transforming inflammatory signals into cancer? Cancer Res. 70, 436–439.
Scala, S., Portella, G., Fedele, M., Chiappetta, G., Fusco, A., 2000. Adenovirus-mediated suppression of HMGI(Y) protein synthesis as potential therapy of human malignant neoplasias. Proc. Natl. Acad. Sci. USA 97, 4256–4261.
Sicinski, P., Donaher, J.L., Geng, Y., Parker, S.B., Gardner, H., Park, M.Y., Robker, R.L., Richards, J.S., McGinnis, L.K., Biggers, J.D., Eppig, J.J., Bronson, R.T., Elledge, S.J., Weinberg, R.A., 1996. Cyclin D2 is an FSH-responsive gene involved in gonadal cell proliferation and oncogenesis. Nature 384, 470–474.
Soule, H.D., Vazquez, J., Long, A., Albert, S., Brennan, M., 1973. A human cell line from a pleural effusion derived from a breast carcinoma. JNCI 51, 1409–1416.
Tan, E.J., Thuault, S., Caja, L., Carletti, T., Heldin, C.H., Moustakas, A., 2012. Regulation of transcription factor twist expression by the DNA architectural protein high mobility group A2 during epithelial-to-mesenchymal transition. J. Biol. Chem. 287 (10), 7134–7145.
Tessari, M.A., Gostissa, M., Altamura, S., Sgarra, R., Rustighi, A., Salvagno, C., Caretti, G., Imbriano, C., Mantovani, R., Del Sal, G., Giancotti, V., Manfioletti, G., 2003. Transcriptional activation of the cyclin A gene by the architectural transcription factor HMGA2. Mol. Cell. Biol. 23, 9104–9116.
Thanos, D., Du, W., Maniatis, T., 1993. The high mobility group protein HMG I(Y) is an essential structural component of a virus-inducible enhancer complex. Cold Spring Harb. Symp. Quant. Biol. 58, 73–81.
Thanos, D., Maniatis, T., 1992. The high mobility group protein HMG I(Y) is required for NF-κB-dependent virus induction of the human IFN-β gene. Cell 27, 777–789.
Trotman, L.C., Niki, M., Dotan, Z.A., Koutcher, J.A., Di Cristofano, A., Xiao, A., Xiao, A., Khoo, A.S., Roy-Burman, P., Greenberg, N.M., Van Dyke, T., Cordon-Cardo, C., Pandolfi, P.P., 2003. Pten dose dictates cancer progression in the prostate. PLoS Biol. 1, E59.
Vallone, D., Battista, S., Pierantoni, G.M., Fedele, M., Casalino, L., Santoro, M., Viglietto, G., Fusco, A., Verde, P., 1997. Neoplastic transformation of rat thyroid cells requires the junB and fra-1 gene induction which is dependent on the HMGI-C gene product. EMBO J. 16, 5310–5321.
Vandenboom Ii, T.G., Li, Y., Philip, P.A., Sarkar, F.H., 2008. MicroRNA and cancer: tiny molecules with major implications. Curr. Genomics 9, 97–109.
Volinia, S., Calin, G.A., Liu, C.G., Ambs, S., Cimmino, A., Petrocca, F., Visone, R., Iorio, M., Roldo, C., Ferracin, M., Prueitt, R.L., Yanaihara, N., Lanza, G., Scarpa, A., Vecchione, A., Negrini, M., Harris, C.C., Croce, C.M., 2006. A microRNA expression signature of human solid tumors defines cancer gene targets. Proc. Natl. Acad. Sci. USA 103, 2257–2261.
Wood, L.J., Maher, J.F., Bunton, T.E., Resar, L.M., 2000. The oncogenic properties of the HMG-I gene family. Cancer Res. 60, 4256–4261.
Wu, J., Liu, Z., Shao, C., Gong, Y., Hernando, E., Lee, P., Narita, M., Muller, W., Liu, J., Wei, J.J., 2011. HMGA2 overexpression-induced ovarian surface epithelial transformation is mediated through regulation of EMT genes. Cancer Res. 71 (2), 349–359.
Xu, Y., Sumter, T.F., Bhattacharya, R., Tesfaye, A., Fuchs, E.J., Wood, L.J., Huso, D.L., Resar, L.M., 2004. The HMG-I oncogene causes highly penetrant, aggressive lymphoid malignancy in transgenic mice and is overexpressed in human leukemia. Cancer Res. 64, 3371–3375.
Zamore, P.D., Haley, B., 2005. Ribo-genome: the big world of small RNAs. Science 309, 1519–1524.